

Vibrational Stark Effects to Identify Ion-Pairing and Determine Reduction Potentials in Electrolyte-Free Environments

Tomoyasu Mani,* David C. Grills, and John R. Miller*

Chemistry Department, Brookhaven National Laboratory, Upton NY 11973-5000, United States

Supporting Information Placeholder

ABSTRACT: A recently-developed instrument for time-resolved infrared detection following pulse radiolysis has been used to measure the $\nu(\text{C}\equiv\text{N})$ IR band of the radical anion of a CN-substituted fluorene in tetrahydrofuran. Specific vibrational frequencies can exhibit distinct frequency shifts due to ion-pairing, which can be explained in the framework of the vibrational Stark effect. Measurements of the ratio of free ions and ion-pairs in different electrolyte concentrations allowed us to obtain an association constant and free energy change for ion-pairing. This new method has the potential to probe the geometry of ion-pairing and allows the reduction potentials of molecules to be determined in the absence of electrolyte in an environment of low dielectric constant.

INTRODUCTION

Ion-pairing is one of the fundamental phenomena in chemistry and biology.^{1,2} Experimental methods such as conductometry and potentiometry exist to measure the strength of ion-pairing, but these methods are usually limited to pairing with metal ions,² and it is difficult to measure ion-pairing between an organic radical ion and an inert non-metal electrolyte. It is of particular interest for chemists to identify ion-pairing of non-metal species as well as to measure reduction potentials in an electrolyte-free environment. For example, in some applications such as organic photovoltaics, we would ultimately like to measure reduction potentials in an electrolyte-free environment of very low dielectric constant ($D_e \sim 2-4$).³ Redox reactions in proteins often occur in hydrophobic nonpolar environments, and these nonpolar environments affect the redox potentials of their active centers,⁴ which underpins the importance of redox chemistry in nonpolar environments. In another arena of chemistry, electron transfer reactions are ubiquitous in organic synthesis, which can be collectively summarized as the “electron is a catalyst” paradigm.⁵ Many reactions can be performed in solvents of a wide range of polarity including nonpolar solvents in the absence of electrolytes. For the development of efficient synthetic methodologies, it is therefore advantageous to determine reduction potentials in environments similar to those in which reactions take place. While electrochemistry using microelectrodes may be applied to measure reduction potentials in an electrolyte-free environment, limitations exist in that it requires modeling of the migration of charges at microelectrodes.⁶

We report here a new method to measure association constants (K_A) for ion-pairing between an organic radical

ion and an electrolyte. The method is based on the vibrational Stark effect (VSE)⁹ that shifts the IR absorption of specific vibrations in response to changes in electric fields. Pulse radiolysis with nanosecond time-resolved infrared (TRIR) detection^{10,11} is newly-developed at the Laser-Electron Accelerator Facility (LEAF) at Brookhaven National Laboratory.¹² Pulse radiolysis, which utilizes a short pulse of high-energy electrons to initiate chemical reactions, confers the ability to produce charged species in the absence and presence of electrolytes with varying concentrations, even in low polarity environments. We used a solvent of moderately low dielectric constant, tetrahydrofuran (THF, $D_e = 7.52$),¹³ in which a dominant reaction after the electron pulse is electron attachment to solutes. As a model molecule, we synthesized 9,9-dihexyl-9H-fluorene-2-carbonitrile (**F1CN**). Radicals of oligofluorenes and polyfluorenes were recently shown to exhibit extremely intense IR absorption bands (ϵ_{max} up to 50,000 $\text{M}^{-1}\text{cm}^{-1}$).¹⁴ However, in this case we introduced the cyano ($-\text{C}\equiv\text{N}$) functional group as an IR-tag because 1) the $\nu(\text{C}\equiv\text{N})$ stretch is known to be responsive to external electric fields^{9,15-17} and ion-pairing with some metals,¹⁸ and 2) we can monitor with relative ease the effects of ion-pairing as the IR absorption of its stretching mode is well separated from other vibrational modes of conjugated molecules such as $\nu(\text{C}=\text{C})$. We show that ion-pairings between an organic radical ion and an inert non-metal electrolyte produce a noticeable VSE in the $\nu(\text{C}\equiv\text{N})$ stretch, allowing us to determine the contributions of free ions and ion-pairs at given electrolyte concentrations. Based on the assumption that the association energy from ion-pairing with a single electrolyte molecule dominates the stabilization of the anions and their energies, we can calculate reduction potentials in an electrolyte-free environment provided the reduction potentials in the pres-

ence of electrolytes can be independently measured by standard electrochemical methods. We also demonstrate the feasibility of determining reduction potentials of non IR-tagged molecules by the measurement of equilibrium constants for bimolecular electron transfer using a reference molecule. The presented method has the potential to probe the geometry of ion-pairing and the reduction potentials of molecules in an electrolyte-free environment of very low dielectric constant.

RESULTS AND DISCUSSION

Vibrational Stark Effects. The synthesis and characterization of **F1CN** are reported in the Supporting Information. An important aspect of the pulse radiolysis technique is its ability to transiently create and observe free ions. Thus, upon pulse radiolysis of a THF solution of **F1CN** in the absence of electrolytes, we observed a red-shifted $\nu(\text{C}\equiv\text{N})$ IR absorption of the free ion (FI) compared to that of the neutral species (Figure 1).

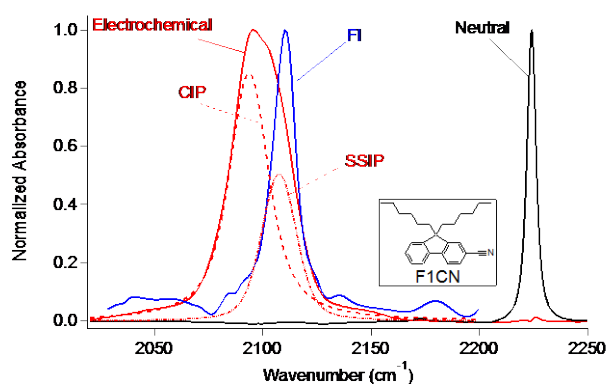


Figure 1. FTIR spectrum of neutral **F1CN** in THF (black), TRIR spectrum of **F1CN**^{•-} free ion (FI) obtained 50 ns after pulse radiolysis of this solution (blue), and FTIR spectrum of the electrochemically-produced ion pair in THF containing 100 mM TBA⁺BF₄⁻ (solid red). The latter can be fit by two Voigt functions that we assign to the contact ion pair (CIP) and the solvent-separated ion pair (SSIP). The inset shows the molecular structure of **F1CN**.

The absorption band of the FI is broader and considerably red-shifted compared to that of the neutral. Both can be fit to single Voigt functions. The extinction coefficient of the FI is also larger ($\epsilon_{\text{max}} \sim 1400 \text{ M}^{-1}\text{cm}^{-1}$ at 2110 cm^{-1}) than that of the neutral ($\epsilon_{\text{max}} \sim 350 \text{ M}^{-1}\text{cm}^{-1}$ at 2224 cm^{-1}). Ion-pairing with tetrabutylammonium (TBA⁺) further shifts the absorption to lower energy (red spectrum in Figure 1). An excellent agreement was obtained between the IR spectra of the electrochemically produced ion pair and that produced radiolytically, both in the presence of 100 mM tetrabutylammonium tetrafluoroborate (TBA⁺BF₄⁻) (Figure S1). From the pulse radiolysis experiments, we determined $\epsilon_{\text{max}} \sim 2650 \text{ M}^{-1}\text{cm}^{-1}$ at 2096 cm^{-1} for the ion-pairs. The extinction coefficients of the $\nu(\text{C}\equiv\text{N})$ stretch of the FI and ion-pairs were determined based on the intensities of the bleach of the $\nu(\text{C}\equiv\text{N})$ stretch of the neutral **F1CN** species in the TRIR spectra.

Spectral shifts by ion-pairing can be explained in the framework of the VSE.⁹ Ion-pairing between the **F1CN**^{•-}

anion and a cation induces an “external” electric field, which shifts and changes the IR absorption of the nitrile stretch. A schematic diagram of the VSE is shown in Figure S2. The shift of the $\nu(\text{C}\equiv\text{N})$ stretch depends on the alignment of the difference dipole moment with the external electric field. The difference dipole moment is defined as the change in dipole moment between the ground ($\nu=0$) and excited ($\nu=1$) state of the vibrational transition of the nitrile. Andrews and Boxer showed that the difference dipole moment points from the nitrogen to the carbon atom parallel to the internuclear bond axis of $\text{C}\equiv\text{N}$.¹⁶ Difference dipole moments stem from a combination of mechanical anharmonicity and electronic perturbations of chemical bonds.^{15,16} The bond length slightly increases in the excited ($\nu=1$) state of the $\nu(\text{C}\equiv\text{N})$ stretch compared to that of the ground state. Because of the anharmonic nature of the potential surface, displacement of charges accompanies the transition; no or a very small VSE is expected when the oscillator is purely harmonic.⁹ This simple picture shows that the energy of the $\nu(\text{C}\equiv\text{N})$ stretch becomes lower (shifts red) when the external positive charge is on the same side of the molecule as the nitrogen atom in the nitrile group; thus, the difference dipole moment is parallel with the external electric field. On the other hand, the energy of the $\nu(\text{C}\equiv\text{N})$ stretch will be higher (blue-shift) when the external positive charge is on the side opposite to the nitrogen atom. Thus, the experimentally observed red-shift of the $\nu(\text{C}\equiv\text{N})$ stretch in ion-pairs indicates that TBA⁺ is positioned on the same side of **F1CN**^{•-} as the nitrile group (Figure S2a). This notion is supported by density functional theory (DFT) calculations. The computed electrostatic potential (ESP) map shows that the nitrile group is the most negatively charged moiety within the molecule (Figure S3), suggesting a positively charged TBA⁺ is likely to be paired with **F1CN**^{•-} on that side. A qualitative agreement of the red-shifting of the $\nu(\text{C}\equiv\text{N})$ stretch was obtained from frequency calculations using DFT at the level of B₃LYP/6-31G(d) (Figure 2).

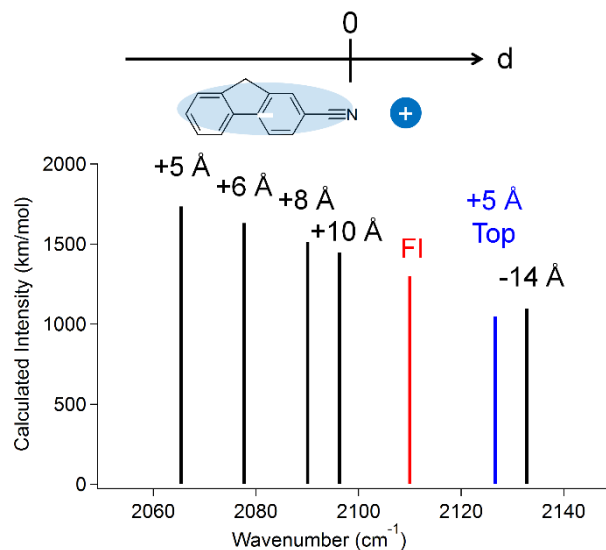
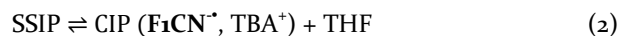


Figure 2. Calculated frequencies of the $\nu(\text{C}\equiv\text{N})$ stretching vibration of F1CN^- . A point charge (+) was positioned at the designated distance from the nitrogen. A clear trend was observed, supporting the interpretation based on the VSE. When a point charge was positioned beside F1CN^- on the same side as the nitrogen, the frequency of $\nu(\text{C}\equiv\text{N})$ was red-shifted. In contrast, the frequency shifted blue- when a point charge was positioned on the opposite side or on the top/bottom of the F1CN^- molecule. The calculated frequency for the FI was scaled to match the experimentally observed frequency. This resulted in a scaling factor of 0.948, which was used for all the other calculated frequencies. Calculated intensities are uncorrected.

The present case is different from well-known examples of LiSCN ,¹⁹ LiSeCN ,²⁰ and inorganic cyanide compounds such as metal cyanide salts,¹⁸ in which ion-pairing results in a blue-shifting of the $\nu(\text{C}\equiv\text{N})$ stretch. Their shifts can also be explained in the framework of the VSE. In the case of LiSCN ,¹⁹ Lee et al., showed “the high frequency CN band mainly results from the S-bound CIP,” which means Li ion is positioned near the S atom and away from the other side of the nitrogen in the nitrile, where the difference dipole moment is aligned anti-parallel to the external electric field produced by the metal cation and cyanide-containing anions (in a similar manner to the case in Figure S2b). We reasoned a blue-shifting of the $\nu(\text{C}\equiv\text{N})$ stretch observed in other salts can be explained similarly.

The spectrum of the ion pair fits to two Voigt functions, pointing to two populations of ion-pairs. We examine the hypothesis that the two populations are the contact ion pair (CIP) and the solvent-separated ion pair (SSIP) (Figure 1). No solvent molecules are present between an anion and a cation in the CIP while there are solvent molecules in the SSIP. The VSE shifts the $\nu(\text{C}\equiv\text{N})$ IR band further in the CIP than in the SSIP as the induced “external” electric field is larger in the CIP. This is supported by the calculations that show a point charge at shorter distance from F1CN^- results in a greater shift of the $\nu(\text{C}\equiv\text{N})$ IR band (Figure 2). The band of the SSIP is slightly red-shifted and broader ($\nu_{\text{max}} = 2108 \text{ cm}^{-1}$, $\text{FWHM} = 19 \text{ cm}^{-1}$) than that of the FI ($\nu_{\text{max}} = 2110 \text{ cm}^{-1}$, $\text{FWHM} = 12 \text{ cm}^{-1}$), which can be clearly identified by pulse radiolysis. The fitting to two Voigt functions becomes poorer when one of the two is fixed as the spectrum of the FI (Figure S4). This points to the possibility that the identified spectra of the SSIP and FI are different, although the difference is admittedly small. Our analysis below is based on the model that assumes 1) we have ion-pairs consisting of CIP and SSIP and 2) the ratio between the CIP and the SSIP does not change with electrolyte concentration. The latter assumption appears to be reasonable as the equilibrium between CIP and SSIP should only be dependent on the concentration of solvent molecules and not on those of individual free ions, based on the following equations



where we set SSIP to have one THF molecule. In addition, we observed the growth of the CIP at 2096 cm^{-1} even at 10

μM of $\text{TBA}^+\text{BF}_4^-$, and the spectrum at each concentration can be fit by the two spectra of the FI and ion-pairs, which supports the assumption. The exact nature of the SSIP (i.e. number of solvent molecules between ions) is an interesting topic, but beyond the scope of the current study. The hypothesis that the ion pair spectrum includes CIP and SSIP is based on the goodness of fittings; a more definite confirmation will require further investigations. Still, our model explains our experimental results well. One alternative model would be to assume that the FI and ion-pairs (possibly only CIP) are present even at 100 mM of $\text{TBA}^+\text{BF}_4^-$ (Figure S4 – the fit with the constraint).

TRIR spectra. We measured TRIR spectra in the $\nu(\text{C}\equiv\text{N})$ stretching region using several different concentrations of $\text{TBA}^+\text{BF}_4^-$ to determine the population ratio of free ions and ion-pairs (Figure 3). The kinetics observed for the decay of the IR absorption matched well with those measured in the UV-Vis region (Figure S5). All anions are free in the absence of electrolyte, and are considered paired with TBA^+ in the presence of 100 mM electrolyte at $\sim 40 \text{ ns}$ after the electron pulse, which is the limit of time resolution of the TRIR detection system at LEAF. This assignment is valid as the spectra obtained radiolytically and electrochemically are almost identical to each other as described above.

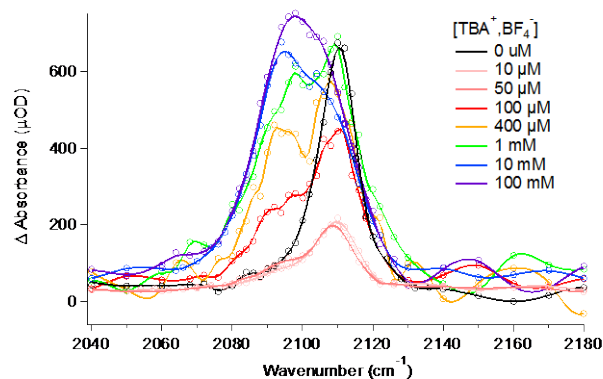


Figure 3. TRIR spectra of F1CN^- obtained 1 μs after pulse radiolysis of THF solutions of F1CN^- ($c \sim 18 \text{ mM}$) containing different concentrations of $\text{TBA}^+\text{BF}_4^-$ (0 μM , 10 μM , 50 μM , 100 μM , 400 μM , 1 mM, 10 mM, and 100 mM). Under these conditions, the concentration of free TBA^+ ions (before ion pairing with F1CN^-) is estimated to be 0, 3.33, 8.33, 12.1, 25.0, 40, 128, and 407 μM , respectively. The spectra with 10 and 50 μM $\text{TBA}^+\text{BF}_4^-$ were obtained 2 μs after pulse radiolysis, and all spectra were normalized for dose fluctuations.

For intermediate electrolyte concentrations (10 μM to 10 mM), free ions present at early times subsequently paired with TBA^+ (Figure S6). The rate constant for ion-pairing between F1CN^- and TBA^+ was determined to be $(2.1 \pm 0.7) \times 10^{11} \text{ M}^{-1}\text{s}^{-1}$ from the kinetic measurements in the five different concentrations of TBA^+ at which we can monitor the growth of the ion-pair’s peak. This value is about one order of magnitude faster than that for a typical diffusion-controlled reaction of two neutral species ($\sim 10^{10} \text{ M}^{-1}\text{s}^{-1}$). This fast rate constant is expected because of Coulomb attraction between F1CN^- and TBA^+ . In THF,

with a dielectric constant of 7.52, Coulomb attraction increases the rate constant by ~ 1 decade by increasing the effective reaction radius to the Onsager radius²¹ of 75 Å. A still faster rate constant ($7.9 \times 10^{11} \text{ M}^{-1}\text{s}^{-1}$)²² was reported for reaction of solvated electrons with Na^+ in THF, where the high diffusion coefficient of the electron further increases the rate. Our observation of an ion-pairing rate constant larger than diffusion-controlled confirms the presence of free ions. Measurement of this rate using UV-Vis detection would have been difficult or impossible due to the broad spectrum of F1CN^- (Figure S5a), but it was enabled by TRIR detection. By 1-2 μs after the electron pulse, an equilibrium between the FI and ion-pairs is established and no further spectral changes are observed. The intensities at lower concentration (10 and 50 μM) are smaller because more free ions decay without being paired up with TBA^+ (Figure S7). Changes at higher concentrations reflect the contributions from the electrolyte dissociation.

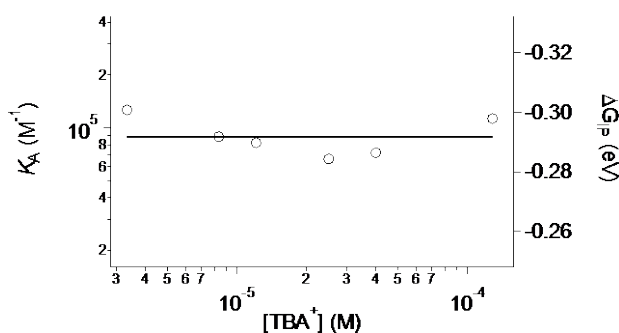


Figure 4. Association constant K_A (M^{-1}) and the free energy change ΔG_{IP} (eV) of the ion-pairing of (F1CN^- , TBA^+) at different concentrations of free TBA^+ . The solid line represents the averages for both K_A and ΔG_{IP} from the six different concentrations. Each point itself is an average determined by two different methods: either by determining the concentrations of each species based on only two wavenumbers or by spectral de-composition.

Figure 4 shows association constants determined from the ratio of ion-pairs/FI for six different concentrations of $\text{TBA}^+\text{BF}_4^-$ by two methods. The mean values from the two methods were used for the subsequent calculations. The ion-pairs/FI ratio ranged from 0.42 at 10 μM to 14.5 at 10 mM $\text{TBA}^+\text{BF}_4^-$. Free ion concentrations of TBA^+ in THF were estimated from the literature values of similar electrolytes (see SI for details).²³ The association constant (K_A) and the free energy change of ion-pairing (ΔG_{IP}) at room temperature were determined to be $(9.2 \pm 2.0) \times 10^4 \text{ M}^{-1}$ and $-0.29 \pm 0.01 \text{ eV}$, respectively for (F1CN^- , TBA^+). This value of K_A lies at the low end of association constants reported for Na^+ or Li^+ with anions of aryl compounds in THF using the conductivity method reported by Szwarc and co-workers.^{24,25} In comparison, $\Delta G_{IP} = -0.31$ and -0.32 eV were reported for (Na^+ , Anthracene $^{\bullet-}$) and (Li^+ , Anthracene $^{\bullet-}$), respectively.^{24,25} The association constant, K_A for (F1CN^- , TBA^+) is about two times smaller than K_A for (Na^+ , Anthracene $^{\bullet-}$) and (Li^+ , Anthracene $^{\bullet-}$). The smaller value for (F1CN^- , TBA^+) is expected because TBA^+ is larger and bulkier in size than small metal ions such as Na^+

and Li^+ , which presumably prevents close contact between the nitrogen center in TBA^+ and an anion.

The reduction potential of F1CN in the presence of 100 mM $\text{TBA}^+\text{BF}_4^-$ was determined to be -2.74 V (vs $\text{Fc}^{+/0}$ in THF) by cyclic voltammetry (Figure S8). With ΔG_{IP} of -0.29 eV , the reduction potential of F1CN in the absence of electrolytes is therefore estimated to be -3.03 V (vs $\text{Fc}^{+/0}$ in THF) (Figure 5). Using pulse radiolysis with visible transient absorption detection, we measured the equilibrium constants for bimolecular electron transfer²⁶ between F1CN and phenanthrene $^{\bullet-}$ (Phen $^{\bullet-}$) in the presence and absence of electrolytes (Table S1). This allowed us to estimate the reduction potential of Phen in the absence of electrolyte using F1CN as a reference molecule (Figure 5).

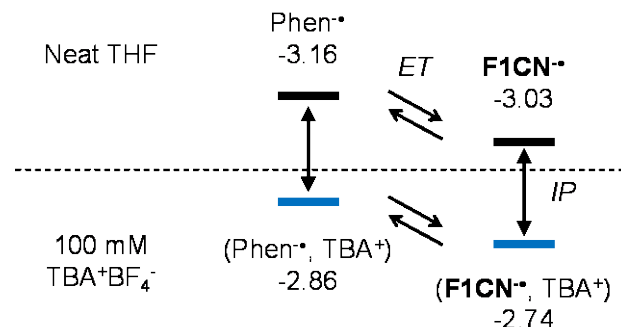


Figure 5. Schematic energy diagram describing the effects of ion-pairing. The values are reported as V vs $\text{Fc}^{+/0}$ in THF. ET and IP stand for electron transfer and ion pairing, respectively.

The reduction potentials of Phen were estimated to be -2.86 V in the presence and -3.16 V in the absence of electrolytes (vs $\text{Fc}^{+/0}$ in THF). The free energy change of the ion-pairing of ($\text{Phen}^{\bullet-}$, TBA^+) is $-0.30 \pm 0.02 \text{ eV}$, similar to that of (F1CN^- , TBA^+). Given the similar size and electron delocalization length of the two anions, the similarity in ion-pairing strength is reasonable. In principle, we can determine reduction potentials of molecules of our interest in the absence of electrolyte as long as equilibria are established for bimolecular electron transfer reactions.

Nature of Ion-Pairing. Our estimate of the reduction potential of F1CN in the absence of electrolyte assumed that the reduction potential in a high concentration of electrolyte (100 mM) is the same as that for a singly-paired ion. This is based on the argument that the major stabilization of anions comes from a single counterion, which is attracted to the anion by the Coulomb (monopole) potential. Additional counter-ions would experience only much weaker ion-dipole attraction (Figure 6a).

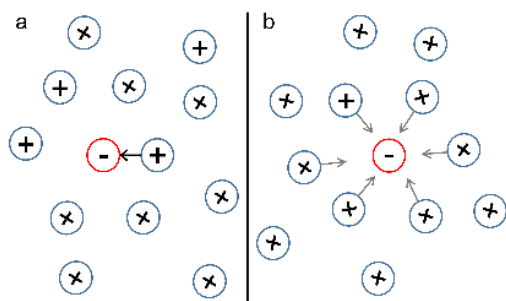


Figure 6. Schematic diagram of ion-pairing in the presence of excess electrolyte. Minus and plus signs represent negative and positive ions, respectively. (a) An anion stabilized dominantly by single ion pairing. (b) An anion stabilized by multiple interactions. Our IR data set supports the former picture.

This view may be counterintuitive and is in contrast to the view that one ion is associated with and stabilized by multiple counter-ions, each of which contributes to stabilization through moderate Coulomb interactions (Figure 6b). In partial support of our argument, we note that the spectrum of ion-pairs at 100 μM $\text{TBA}^+\text{BF}_4^-$, obtained by subtracting the FI contribution, agrees with that obtained at 100 mM $\text{TBA}^+\text{BF}_4^-$, within experimental error ($\sim 10\%$) as shown in Figure S9. If the picture of Figure 6b were correct, the IR spectrum in the presence of 100 mM $\text{TBA}^+\text{BF}_4^-$, should not be the same as that for single ion pairs. The IR results thus support the idea, depicted in Figure 6a, that a radical anion in 100 mM of $\text{TBA}^+\text{BF}_4^-$, pairs principally with one TBA^+ counter-ion; having only loose association with other TBA^+ ions. The IR results thus give new insight into the nature of electrolyte solutions commonly used to determine redox potentials. They also suggest that radical ions in 100 mM electrolyte are similar to the ion-pairs formed in dilute solutions of electrolyte, supporting the estimate that the redox potential changes little after formation of ion-pairs. The reduction potentials in the absence of electrolytes reported here are thus considered to be lower limits. At present we have no method to definitively determine what we suspect is a small difference between redox potentials with a single ion pair vs. the redox potential in 100 mM electrolyte, but we will seek such a method in the future.

CONCLUSION

In conclusion, we report a new method, utilizing pulse radiolysis with TRIR detection, to determine association constants between an organic radical and an electrolyte, taking advantage of the VSE. While association constants are known for the pairing of radical ions with alkali metals like Na^+ , those methods^{24,25} are not applicable to counter ions like TBA^+ that is are commonly used in electrochemistry. The TRIR results suggest that radical anions in the 100 mM electrolyte solutions commonly used for electrochemistry resemble single ion pairs and may be principally paired with one counterion. Within what we expect is a small error. The IR method can determine reduction potentials in an electrolyte-free environment when the

potentials are known in the presence of electrolyte by standard electrochemical methods. Furthermore, we demonstrated the feasibility of determining reduction potentials of non IR-tagged molecules by the measurement of equilibrium constants for bimolecular electron transfer using a reference molecule. This in turn allows us to estimate strengths of ion-pairings between a wide range of molecules and an electrolyte. The presented method has the potential to probe the geometry of ion-pairing and the reduction potentials of molecules in an electrolyte-free environment of very low dielectric constant.

ASSOCIATED CONTENT

Supporting Information. Experimental methods including the synthesis and characterizations of F1CN , Figures S1-S9, and ^1H and ^{13}C NMR spectra of F1CN . This material is available free of charge via the Internet at <http://pubs.acs.org>.

AUTHOR INFORMATION

Corresponding Author

* tmani@bnl.gov and jrmiller@bnl.gov

ACKNOWLEDGMENT

This material is based upon work supported by the U.S. Department of Energy, Office of Science, Office of Basic Energy Sciences through Grant DE-AC02-98-CH10886, including use of the LEAF facility of the BNL Accelerator Center for Energy Research and the computer Cluster at the Center for Functional Nanomaterials. T.M. is grateful for the support by the Goldhaber Distinguished Fellowship from Brookhaven Science Associates. The authors thank Bobby H. Layne for technical assistance in LEAF experiments and Dr. Qin Wu for his assistance in quantum calculations.

REFERENCES

- (1) Szwarc, M. *Accounts Chem. Res.* **1969**, *2*, 87.
- (2) Marcus, Y.; Hefter, G. *Chem. Rev.* **2006**, *106*, 4585.
- (3) Clarke, T. M.; Durrant, J. R. *Chem. Rev.* **2010**, *110*, 6736.
- (4) Moore, G. R.; Pettigrew, G. W.; Rogers, N. K. *Proc. Natl. Acad. Sci. U.S.A.* **1986**, *83*, 4998.
- (5) Studer, A.; Curran, D. P. *Nat. Chem.* **2014**, *6*, 765.
- (6) Oldham, K. B.; Feldberg, S. W. *J. Phys. Chem. B* **1999**, *103*, 1699.
- (7) Bond, A. M.; Feldberg, S. W. *J. Phys. Chem. B* **1998**, *102*, 9966.
- (8) Bond, A. M. *Analyst* **1994**, *119*, R1.
- (9) Boxer, S. G. *J. Phys. Chem. B* **2009**, *113*, 2972.
- (10) Grills, D. C.; Farrington, J. A.; Layne, B. H.; Lyman, S. V.; Mello, B. A.; Preses, J. M.; Wishart, J. F. *J. Am. Chem. Soc.* **2014**, *136*, 5563.
- (11) Grills, D. C.; Cook, A. R.; Fujita, E.; George, M. W.; Preses, J. M.; Wishart, J. F. *Appl. Spectrosc.* **2010**, *64*, 563.
- (12) Wishart, J. F.; Cook, A. R.; Miller, J. R. *Rev. Sci. Instrum.* **2004**, *75*, 4359.
- (13) *CRC Handbook of Chemistry and Physics*; 93rd ed.; Haynes, W. M., Ed.; CRC Press, 2012.
- (14) Zamadar, M.; Asaoka, S.; Grills, D. C.; Miller, J. R. *Nat Commun* **2013**, *4*, 2818 1.
- (15) Andrews, S. S.; Boxer, S. G. *J. Phys. Chem. A* **2002**, *106*, 469.

- (16) Andrews, S. S.; Boxer, S. G. *J. Phys. Chem. A* **2000**, *104*, 11853.
- (17) Baiz, C. R.; Kubarych, K. J. *J. Am. Chem. Soc.* **2010**, *132*, 12784.
- (18) Gill, J. B. *Pure Appl. Chem.* **1981**, *53*, 1365.
- (19) Lee, K. K.; Park, K. H.; Kwon, D.; Choi, J. H.; Son, H.; Park, S.; Cho, M. *J. Chem. Phys.* **2011**, *134*, 064506
- (20) Park, K. H.; Choi, S. R.; Choi, J. H.; Park, S.; Cho, M. *Chemphyschem* **2010**, *11*, 3632.
- (21) Warman, J. M. In *The Study of Fast Processes and Transient Species by Electron Pulse Radiolysis*; Baxendale, J. H., Busi, F., Eds.; D. Reidel: Dordrecht, Holland, 1982, p 433.
- (22) Bockrath, B.; Dorfman, L. M. *J. Phys. Chem.* **1973**, *77*, 1002.
- (23) LeSuer, R. J.; Buttolph, C.; Geiger, W. E. *Anal. Chem.* **2004**, *76*, 6395.
- (24) Nicholls, D.; Sutphen, C.; Szwarc, M. *J. Phys. Chem.* **1968**, *72*, 1021.
- (25) Slates, R. V.; Szwarc, M. *J. Phys. Chem.* **1965**, *69*, 4124.
- (26) Takeda, N.; Asaoka, S.; Miller, J. R. *J. Am. Chem. Soc.* **2006**, *128*, 16073.

Table of Contents

